Neutron-Scattering Studies of the Structure of Highly Tetrahedral Amorphous Diamondlike Carbon

P. H. Gaskell and A. Saeed
Cavendish Laboratory, University of Cambridge, Madingley Road, Cambridge CB3 0HE, United Kingdom

P. Chieux
Institut Laue-Langevin, 156 X, F-38042 Grenoble CEDEX, France

D. R. McKenzie
School of Physics, University of Sydney, New South Wales 2006, Australia
(Received 22 April 1991)

The structure of *a*-C prepared by plasma-arc deposition has been determined by neutron scattering and analyzed to estimate the fraction of tetrahedrally and trigonally bonded carbons. The structure factor and reduced radial distribution functions are similar to those for *a*-Si and *a*-Ge, indicating a high proportion of tetrahedral bonding. Also, the mean value of the nearest-neighbor C-C distance is close to that of crystalline diamond and a fit to the data gives about 86% tetrahedral bonding. This form of diamondlike carbon therefore appears to be the structural equivalent of *a*-Si and *a*-Ge.

PACS numbers: 61.12.Ex, 61.55.Dc

There is considerable interest in the structure and properties of a family of materials often known as amorphous "diamondlike" carbon (*a*-DLC). Films can be insulating, optically transparent, hard, and chemically inert and applications range from protective coatings for semiconductor optics to blood-compatible coatings in artificial hearts and hip-joint prostheses. Structurally, these materials are unusual in that carbon exhibits variable proportions of two hybridization states—corresponding to tetrahedral and trigonal bonding—often associated with different concentrations of hydrogen. We report here a determination by neutron scattering of the structure of a form of diamondlike carbon that closely resembles the structures of the other amorphous tetrahedral elemental semiconductors, silicon and germanium.

The films were prepared using a filtered dc vacuum arc technique similar to that described by Aksenov *et al.* [1]. An arc is struck at a base pressure of 1.3×10^{-4} Pa on a graphite cathode. A magnetic field confines the arc to a circular path on the cathode giving a plasma consisting of neutral and ionized C, and graphite macroparticles. A solenoidal magnetic field acting along the length of a curved drift tube filters out most of the macroparticles and neutral species [2]. The energy of the carbon ions at the filter exit is around 22 eV.

A 20–30-mg specimen was prepared by repeated deposition onto a glass substrate. Although minute by the standards of specimen masses normally used in neutron scattering, careful adjustment of the specimen in the neutron beam and the excellent stability of the twin-axis diffractometer (D4, at the Institut Laue-Langevin, Grenoble) allowed relatively good statistics in a counting time of 32 h. Measurements were made to a maximum scattering vector, $Q_{\max}=4\pi(\sin\theta_{\max})/\lambda=163$ nm^{-1}, where 2θ is the scattering angle and λ is the neutron wavelength (0.0703 nm).

After applying standard corrections for container, self-absorption, multiple, and inelastic scattering, a pronounced decrease in intensity was observed at higher values of Q: a problem usually associated with the presence of hydrogen. Assuming that the H contribution to the scattered intensity has a Q dependence similar to that given by Chieux, deKouchkovsky, and Boucher [3], the H content can be estimated by requiring that $Q^2[S(Q)-1]$ oscillate around zero: A H content of about 11 at.% is indicated. [$S(Q)$ is the structure factor.] Measurement of the H content in a 400-μg specimen was also made using microcombustion analysis [4] and gave a value of 2.5–5 at.% H; the uncertainty is large because of the small amount of H and the limited specimen mass. As shown later, uncertainty in the concentration of hydrogen and the possibility of well-defined C-H correlations provide a limitation to the information available from the scattering data. As a first approximation, however, H is simply treated as a chemically inactive impurity and, after subtraction of the H scattering, the resultant data are processed as a pure C specimen. Normalization of the differential cross section was achieved using the Krogh-Moe–Norman [5,6] self-normalization method. A cruder self-normalization was also used by taking the scattering at $Q=160$ nm^{-1}, an apparent node of the oscillations, as the sample total scattering level, an approach that directly gives a value for the (carbon) atomic density of 1.7×10^{29} m^{-3}.

Estimates of the atomic density were also obtained from the energy E_p (in eV) of the plasmon peak [7,8] observed by electron energy-loss spectroscopy (EELS) at 31 eV, using $E_p=\hbar(N/\varepsilon_0 m^*)^{1/2}$. Here, $m^*=0.9$ is an effective mass chosen so that EELS data for diamond is consistent with the density ρ. This gives a value of the electron density, $N=6.29\times10^{29}$ m^{-3}. Since C and H contribute four and one electrons, respectively, to the valence-electron plasmon, the atomic density n can be calculated, assuming a composition of $C_{0.89}H_{0.11}$. Thus,

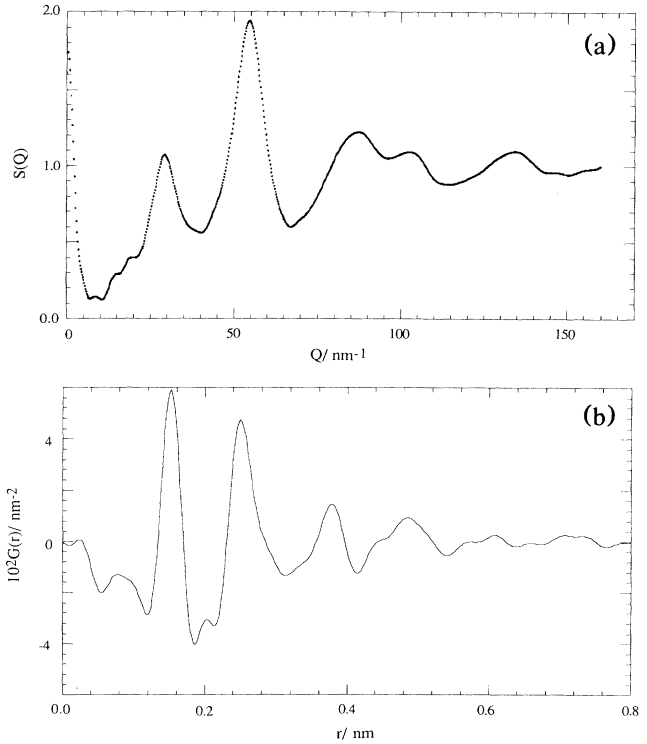

FIG. 1. (a) The structure factor $S(Q)$ for amorphous diamondlike carbon. (b) The reduced radial distribution function $G(r)$ obtained by Fourier transformation of $Q[S(Q)-1]$ to $Q_{max}=160$ nm^{-1}.

$4n_C+n_H=N=6.29\times10^{29}$ with $n_C/n_H=0.89/0.11$, giving $n_C=1.53\times10^{29}$ m^{-3}, $n_H=0.19\times10^{29}$ m^{-3}, $n=1.71\times10^{29}$ m^{-3}, and $\rho=3070$ kgm^{-3}. These values are reasonably close to the density measured by Swift [9] (3000 kgm^{-3}) using an immersion technique and assuming a 10% void fraction. Thus, the bulk density of the specimen lies within 13% of the density of crystalline diamond (3520 kgm^{-3}) and the atomic density is about 97% of that for crystalline diamond (1.765×10^{29} m^{-3}).

The structure factor $S(Q)$ is shown in Fig. 1(a). $Q[S(Q)-1]$ data were Fourier transformed to obtain the reduced radial distribution function $G(r)$ [Fig. 1(b)] without employing any modification function. Here, $G(r)=4\pi n_C r[g(r)-1]$ with

$$g(r)=1+(2\pi^2 n_C r)^{-1}\int_0^\infty Q[S(Q)-1]\sin Qr\,dQ\,.$$

$G(r)$ was fitted by a series of δ functions at distances R_j and with weights N_j corresponding to the coordination numbers of the jth-neighbor shell. These were broadened by Gaussians and convoluted with a real-space peak shape function (a Bessel function J_0) corresponding to termination of the Fourier transform at $Q_{max}=160$ nm^{-1}, thus simulating the effects of truncation of the Q-space data.

A fit to $G(r)$ for a-DLC is shown in Fig. 2 and the fitting parameters given in Table I. The choice of N and σ for each peak and the arbitrary division of the second peak into component Gaussians are all strongly correlated. Tests with alternative fitting criteria suggest that the least reliable parameters are the coordination numbers and the σ values—particularly those corresponding to the second peak, where the positioning of the shoulder at 0.28 nm affects the detail. Results are given for two values of n_C corresponding to EELS data and the fit to the neutron data. Experimental $G(r)$ data for crystalline diamond, measured under identical experimental conditions, has

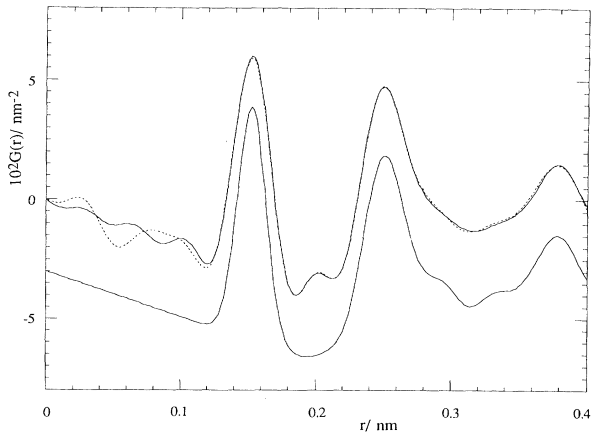

FIG. 2. A fit to the $G(r)$ data shown in Fig. 1(b) using the parameters given in Table I (with $n_C=1.53\times10^{29}$ m^{-3}). In the upper part of the diagram, the experimental data (dotted curve) is compared with a sum of Gaussian contributions (solid curve) convoluted with a peak shape function (a Bessel function J_0) corresponding to termination of the Fourier transform at $Q_{max}=160$ nm^{-1}. The lower part of the diagram (displaced by three units) shows the sum of Gaussian components before convolution, and this gives a more realistic impression of the detailed structure underlying $G(r)$.

TABLE I. Mean interatomic distances $\langle r\rangle$, standard deviation σ, and coordination number N, obtained by fitting experimental $G(r)$ data for a-DLC ($n_C=1.53\times10^{29}$ m^{-3}). Figures in parentheses for a-DLC indicate values of N and σ calculated with $n_C=1.68\times10^{29}$ nm^{-3}. Parameters for the fit to scattering data for diamond recorded under the same experimental conditions are also given. The subscripted figure is only marginally significant.

a-DLC			Crystalline diamond		
$\langle r\rangle$ (nm)	N	σ (nm)	$\langle r\rangle$ (nm)	N	σ (nm)
0.152_6	3.93 (4.26)	0.011 (0.011_5)	0.153_6	4.0	0.004_3
0.211	0.22 (0.50)	0.011 (0.011_5)			
0.250_0	8.90 (9.30)	0.016	0.252_2	12.0	0.006_3
0.275	2.05 (2.60)	0.014			
0.296_0	4.05 (4.40)	0.014	0.296_2	12.0	0.004_7
0.329_5	5.70 (6.50)	0.016			
0.355_4	3.00 (3.40)	0.016	0.355_7	6.0	0.004_5
0.382	15.2 (16.50)	0.020	0.387_7	12.0	0.004_1

also been fitted and can be used to standarize the data for the amorphous material. The first three peaks were shifted slightly (less than 0.001 nm) from literature values.

The position of the first peak (0.152_6) in *a*-DLC is close to that for crystalline diamond (0.153_6). It is distinctly different from the literature value for graphite (0.1421 nm). This is also true of the position of the second peak at 0.250 nm, compared with 0.252_2 measured for diamond. These distances are insensitive (to better than 2×10^{-3} nm) to the various assumed material parameters and to reasonable changes in $Q_{\max}$—in contrast to absolute coordination numbers which are strongly correlated with the H content and density values.

We have synthesized the detailed shape of the first peak in $G(r)$ using a mixture of C-C distances in diamond and graphite. The fraction of graphitic C was varied from 0% to 20% and the fraction of diamondlike, sp^3, carbon is found to be about 86%, with a lower limit of 80%; see Fig. 3. These figures are in good agreement with estimates based on the intensity of the $1s\rightarrow 2\pi^*$ EELS transition [10]. The validity of the assumption that H is present as a noninteracting impurity is shown by the absence of a strong (negative) contribution at 0.11 nm associated with C-H distances. Infrared absorption spectroscopy also failed to detect any C-H bonding.

The standard deviation σ_1 for the first-shell distribution given in Table I includes the effect of thermal (σ_1^t) as well as static disorder (σ_1^s) arising from fluctuations in C-C distances. The latter term can be estimated using

$$\sigma_1^s=[(\sigma_1)^2-(\sigma_1^t)^2]^{1/2} \text{ or } \sigma_1^s=[(\sigma_1)^2-(\sigma_1^c)^2]^{1/2},$$

where σ_1^c refers to the crystal (with no static broadening). Thermal broadening is assumed to be equivalent in the amorphous and crystalline phases, reflecting observed similarities between the vibrational density of states of crystalline and amorphous forms of Si and Ge. The value of σ_1^s is larger than that observed in either *a*-Si or Ge.

The second peak has been modeled by two Gaussians, the strongest being centered at 0.25 nm. A bond angle of $110.0°\pm0.3°$ is obtained if this peak alone is assigned as a second-neighbor distance. Taking a weighted mean of the contributions at 0.25 and 0.275 nm leads to a bond angle of 113°.

Accurate estimation of the *absolute* values of first- and second-shell coordination numbers presents difficulties due to uncertainties in values of several material constants. On the other hand, the *relative* magnitude of first- and second-neighbor contributions is reasonably insensitive to the assumed material constants. The ratio N_2/N_1 is 2.8 (to about 5%): Values of 3.0 and 2.0 characterize fully bonded tetrahedral and trigonal networks, respectively.

The structural parameters quoted in Table I distinguish, quite clearly, this material from others examined recently by scattering techniques. Honeybone *et al.* [11] have measured the neutron $S(Q)$ for *a*-C containing about 30% H and find peaks in $G(r)$ at 0.139 and 0.152 nm in the ratio 1:4 with $N_1=2.5\pm1.0$ and $N_2=4.0\pm2.0$ atoms. Also, Li and Lannin [12] reported neutron-scattering data for *a*-C with $\rho\approx2000$ kg m^{-3}, and find a first peak at 0.146 nm with $N_1=3.34$ and a bond angle of 117°.

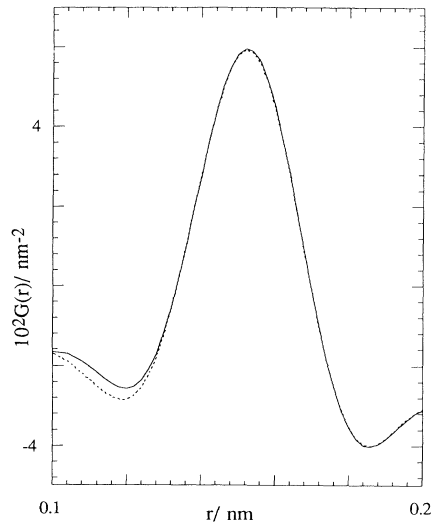

FIG. 3. Experimental first peak distribution, corresponding to Fig. 1(b), fitted with a weighted sum of Gaussian contributions centered at interatomic distances corresponding to crystalline diamond and graphite. The dotted line represents experimental data and the solid line represents the fitted curve with 14% graphitic bonding.

The material examined here is more akin to other amorphous elemental tetrahedral semiconductors, as comparison of $S(Q)$ or $G(r)$ with data for *a*-Ge or *a*-Si makes plain. The discrepancy between the ratio of N_2 and N_1 determined from this experiment and that expected for a tetrahedral network deserves comment. For a fully bonded network with $N_1=m$, $N_2=m(m-1)$ and $N_2/N_1=m-1$. This experiment suggests that a reasonable estimate for N_1 would be 3.8 [13]. Comparison of the measured first-neighbor distribution with data for diamond and graphite indicates a predominantly tetrahedral network with about 14% trigonal bonding corresponding to $N_2/N_1=2.9$ and $m=3.9$, whereas $m=3.8$ would imply about 24% trigonal bonding. However, allowing for some broken C-C bonds due to disorder and C-H bonding, a value for $m=3.8$ probably lies within the bounds of error of the measurement.

This is an upper limit, though, based on the assumption that the contribution at 0.275 nm is all due to second neighbors, although some third-neighbor contribution could be expected. Only a three-dimensional space-filling model can give a reliable analysis, but by analogy with Temkin's model for *a*-Ge [14], about 75% of the 0.275-nm distribution may be due to third neighbors, giving

$m = 3.4$. But this is excluded if all the trigonal bonds have a bond length equivalent to graphite. A possible explanation may be that a fraction of the C-C bonds possess bond lengths close to diamond yet have the nearest-neighbor connectivity of graphite. The suggestion is not so radical: Compression of the graphite lattice parallel to the hexad axis is known to lead to crystallographic transformations to a hexagonal form of carbon [15]. Moreover, it has been proposed that the highly tetrahedral structure of these films results from compressive stresses generated by shallow implantation of C ions during deposition [16]. What is suggested here is that a fraction of the amorphous lattice may be converted to an intermediate state with one long "bridging" C-C bond at a distance greater than 0.2 nm, and three C-C bonds that are best described as sp^3 since the bond angle is close to 109° and the length near that of diamond. [A perfect fit to $G(r)$ requires 0.2–0.4 atom at 0.21 nm, which may be significant.] These suggestions are compatible with the calculations of the atomic motions involved in the transition from "rhombohedral" graphite to diamond [17], and cross-linking between essentially graphitic layers is implicit in the recent work of Tamor and Wu [18] and Gao *et al.* [19] although these models imply essentially graphitic bonding throughout.

While the experimental data are far from satisfactory due to the limited specimen mass, we believe that the most important result is not seriously affected by experimental uncertainty. This is that the most appropriate description of this type of amorphous carbon is in terms of tetrahedral bonding but with a significant fraction of the atoms having a connectivity characteristic of trigonal bonding, as in graphite.

P.H.G. acknowledges the generous financial support of Pilkington Brothers Plc. We are grateful to P.D. Swift for specimen preparation, K.W.R. Gilkes and J. Robertson for useful discussions, and to Professor C. Pillinger, Open University, United Kingdom for the hydrogen analysis.

[1] I. I. Aksenov, V. A. Belous, V. G. Padalka, and V. M. Khoroshikh, Fiz. Plazmy **4**, 758 (1978) [Sov. J. Plasma Phys. **4**, 425 (1978)]; J. Franks, in *Diamond and Diamond-like Films and Coatings,* edited by R. E. Clausing, L. L. Horton, J. C. Angus, and P. Koidl (Plenum, New York, 1991).

[2] D. R. McKenzie, P. J. Martin, S. B. White, Z. Liu, W. G. Sainty, D. J. H. Cockayne, and D. M. Dwarte, in *Proceedings of the European Materials Research Society Conference, Strasbourg, 1987,* edited by P. Koidl and P. Oelhafen (1988), p. 203.

[3] P. Chieux, R. deKouchkovsky, and B. Boucher, J. Phys. F **14**, 2239 (1984).

[4] C. Pillinger (private communication).

[5] J. Krogh-Moe, Acta Crystallogr. **9**, 951 (1956).

[6] N. Norman, Acta Crystallogr. **10**, 370 (1957).

[7] R. F. Egerton, *Electron Energy Loss Spectroscopy in the Electron Microscope* (Plenum, New York, 1986), p. 152.

[8] T. Miyazawa, S. Misawa, S. Yoshida, and S. Gonda, J. Appl. Phys. **55**, 188 (1984).

[9] P. D. Swift, Ph.D. thesis, University of Sydney, Australia (unpublished).

[10] S. D. Berger and D. R. McKenzie, Philos. Mag. Lett. **57**, 285 (1988).

[11] P. J. R. Honeybone, R. J. Newport, W. S. Howells, and J. Franks, in Proceedings of the NATO Advanced Study Institute, Pisa, 1990, edited by C. McHargue (Plenum, New York, to be published).

[12] F. Li and J. S. Lannin, Phys. Rev. Lett. **65**, 1905 (1990).

[13] A similar value is observed by filtered electron diffraction [D. Muller (private communication)].

[14] R. J. Temkin, J. Non-Cryst. Solids **28**, 23 (1978).

[15] F. B. Bundy and J. S. Kaspar, J. Chem. Phys. **46**, 3437 (1967).

[16] D. R. McKenzie, D. Muller, and B. A. Pailthorpe, Phys. Rev. Lett. **67**, 773 (1991).

[17] S. Fahy, S. G. Louie, and M. H. Cohen, Phys. Rev. B **34**, 1191 (1986).

[18] M. A. Tamor and C. H. Wu, J. Appl. Phys. **67**, 1007 (1990).

[19] C. Gao, Y. Y. Wand, A. L. Ritter, and J. R. Dennison, Phys. Rev. Lett. **62**, 945 (1989).